THE INTEGRATED
MANUAL AND AUTOMATIC CONTROL
OF COMPLEX FLIGHT SYSTEMS

Semi-Annual Status Report

for the Period July 1, 1982 - Dec. 31, 1982

Principal Investigator: Dr. David K. Schmidt
School of Aeronautics & Astronautics
Purdue University
West Lafayette, IN 47907

NASA Technical Officer: Mr. Donald T. Berry
Vehicle Dynamics and Control Division
Ames Research Center
Dryden Flight Research Facility
P.O. Box 273
Edwards, CA 93523

Grant No. NAG4-1

March 3, 1983

1. Introduction

This constitutes the semi-annual status report for the period July 1, 1982 - Dec. 21, 1982, on the research being performed by the School of Aeronautics and Astronautics, Purdue University, for the NASA Dryden Flight Research Facility, Ames Research Center, under Grant NAG4-1. The objective of this research effort has been the development of a unified control synthesis methodology for complex and/or non-conventional flight vehicles, and to understand, enhance, and develop prediction techniques for the handling characteristics of such vehicles.

2. Publications, Personnel and Discussion

Two papers were presented at the 1982 AIAA Atmospheric Flight Mechanics, and Guidance and Control Conferences in San Diego in August, 1982, on results obtained under this grant. These papers were

1. "Application of An Optimal Cooperative Control Technique for Augmentation Synthesis of a Control Configured Aircraft," by Mario Innocenti and David K. Schmidt, presented at the Guidance and Control Conference AIAA Paper No. 82-1520.

2. "A Modern Approach to Pilot/Vehicle Analysis and the Neal-Smith Criteria," by Barton J. Bacon and David K. Schmidt, presented at the Atmospheric Flight Mechanics Conf., AIAA Paper No. 82-1357.

In addition, the material documented in NASA CR 163112, entitled Pilot-Orientation Multivariable Control Synthesis by Output Feedback was submitted over a year ago for possible publication in the AIAA Journal of Guidance, Control and Dynamics. The reviewers comments have been received during this reporting period, with their recommendation that the paper be accepted for publication after the material in paper 1) above is added to the manuscript. This is currently being accomplished and we are eager to have these results appear in a journal article.

Also, paper 2) above was submitted as well for journal publication. The reviewers have recommended that this paper appear after only minor revision in the Journal of Guidance, Control and Dynamics. This has been accomplished, and we look forward to its appearance.

Finally, a paper has just been completed, and will be presented at the 1983 IEEE National Aerospace and Electronics Conference (NAECON), Dayton, OH, May 1983. This paper is entitled

> "Integrated Pilot-Optimal Augmentation Synthesis for Complex Flight Systems: Experimental Validation," by Mario Innocenti and David K. Schmidt.

This last paper documents the experimental validation of the analytical predictions of the handling characteristics of several sets of augmented vehicle dynamics. Copies of the manuscripts for all the papers cited above have been previously forwarded to the Technical Monitor.

With the graduation of Mario Innocenti in December, 1983, extensive development of the cooperative control synthesis theory is complete, and future activities will most likely focus on application of the methodology to a variety of areas.

The research on pilot model identification and on extending the Neal-Smith approach is progressing well. Mr. Pin-Jar Yuan is developing several approaches to pilot model identification, extending the work in this area that has been reported on in several previous papers. The status on this work is completely documented in the Appendix to this report.

The investigation of the potential of extending the optimal-control approach to Neal/Smith analysis for the approach and landing task is the final area of research currently being pursued. This work is being performed by Mr. Bart Bacon, the co-author of our paper on the method, and

Mr. Dan Garrett, a new student now supported on this grant. Mr. Garrett is an M.S. student and is planning to graduate in December, 1983. This topic area will constitute his M.S. thesis.

Ph.D Proposal

"Identification of Pilot Dynamics and Task Objectives from Man-in-the-Loop Simulation"

APPENDIX

by

Pin-Jar Yuan

Purdue University
School of Aeronautics and Astronautics

Dec. 13 1982

Index

Abstract

The objective of this research is to develop a useful and meaningful technique for identification of pilot dynamics and objectives, using both time domain and frequency domain methods. Simulation data generated with a human in the loop will be used. We introduce this with a simple example; a single input pursuit task, and it can be extended to general piloted vehicle tasks from single input tracking task to multi-input complex task, for example, landing approach.

1. Background

1.1. Introduction

In the late 60's, the optimal control model (OCM) of the pilot was developed, which is based on the hypothesis that a human operator (pilot) chooses his control input to minimize some cost function subject to his known physical limitation. The OCM of the human operator has yielded results for the manual control of a variety of plants that agree with experimental findings provided that the correct cost function is assumed (Ref. 1).

Later, Hess (Ref. 2) showed that there exists a strong correlation between the subjective pilot evaluation (e.g. Cooper-Harper rating) of the vehicle and the magnitude of the OCM quadratic cost function. Recent investigations (Ref. 3) have provided more substance to the idea that such a correlation exists over a wider variety of piloted vehicle tasks. The above correlation between the pilot rating and the OCM objective function has been used by Schmidt (Ref. 4,5) in the attempt to develop a unified theory of vehicle handling qualities and optimal flight control synthesis.

1.2. Model structure

The analysis relies on the well-known (Ref. 1) optimal control theoretic technique for modeling the human pilot manual control function. The hypothesis upon which it is based is that the well trained, well motivated pilot chooses

his control inputs (e.g. stick force) to meet the pilot's mission objective, which can be described as minimizingg a meet the pilot's mission objective, which can be described as minimizing a suitable cost function in the task, subject to his human limitations. The cost function is further assumed to be expressible in terms of a quadratic form as following:

$$J = E\left\{ \lim_{t\to\infty} \frac{1}{t} \int_0^t \left(y^T Q y + u^T R u \right) dt \right\} \qquad (1.1)$$

where

y = vector of pilot's observed variables
u = vector of pilot's control inputs
Q,R = pilot selected weightings

and the pilot model is sketched briefly in Figure 1-1. The human pilot chooses his "best" control decision (for example stick force) based on the information displayed to him (pilot observations) and the performance objective reference. So the suitable selection of cost function is very important in representing the human pilot. And in this pilot model, we include the human limitation such as information-acquision, time delay, observation and control output noises, and neuromuscular dynamics etc..

The pilot perceives measurable variables y delayed a fixed time τ , and contaminated by white observation noise v_y . So his measurement vector y_p is

$$y_p(t) = y(t-\tau) + v_y(t-\tau) \qquad (1.2)$$

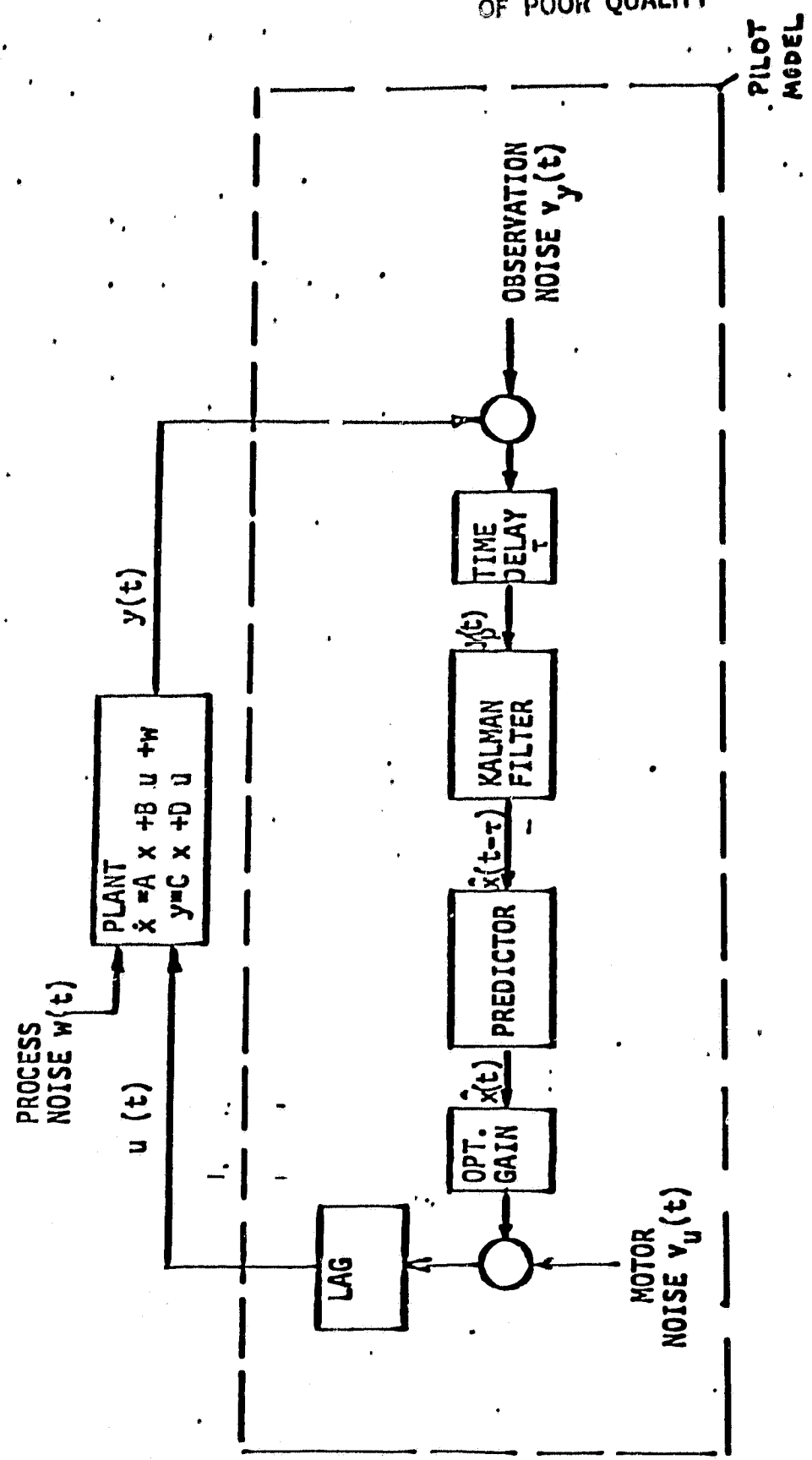

Fig. 1-1
Optimal Control Pilot Model

The pilot neuromotor dynamics can be represented approximately by an adjustable first order lag ($\frac{1}{\tau_n s+1}$), generated naturally in the modeling by including the control rate as the "input" to be chosen to minimize the cost function (see equ. (1.1)). The augmented state equations then become

$$\dot{x}(t) = A_o\, x(t) + B_o\, \mu(t) + w_o(t) \qquad (1.3)$$

with

$$x = \begin{vmatrix} x \\ u \end{vmatrix}$$

$$A_o = \begin{vmatrix} A & B \\ 0 & 0 \end{vmatrix}$$

$$B_o = \begin{vmatrix} 0 \\ 1 \end{vmatrix}$$

$$w_o(t) = \begin{vmatrix} w(t) \\ 0 \end{vmatrix} \qquad (1.4)$$

It can be shown in this case that the optimal control μ (=$\dot{u}$) is the linear feedback law

$$\mu(t) = G\, \hat{x}(t) \qquad (1.5)$$

where $G = [\, G_x \,,\, G_u \,]$, or equivalently

$$\tau_n\, \dot{u}(t) + \hat{u}(t) = L\, \hat{x}(t) = u_c(t) \qquad (1.6)$$

where $\tau_n = \frac{-1}{G_u}$; $L = \tau_n\, G_x$, and $\hat{x}(t)$ is the estimate of state $x(t)$. The feedback gain G is

$$G = -R^{-1}\, B_o^T\, K_o \qquad (1.7)$$

where K_o satisfies the Riccati equation

$$A_0^T K_0 + K_0 A_0 + Q_0 - K_0 B_0 R^{-1} B_0^T K_0 = 0 \qquad (1.8)$$

in which

$$Q_0 = \begin{vmatrix} C^T Q C & 0 \\ 0 & 0 \end{vmatrix}$$

The state estimator consists of a Kalman filter and predictor, and the effect of the motor noise $v_u(t)$ is included. We define as before the augmented state $x(t)$ =col $[x(t), u(t)]$ which satisfies

$$\dot{x}(t) = A_1 x(t) + B_1 u_c(t) + w_1(t) \qquad (1.9)$$

in which $w_1(t)$ = col $[\, w(t) \,,\, \frac{v_u(t)}{\tau_n} \,]$, B_1 = col $[\, 0 \,,\, \frac{1}{\tau_n} \,]$, and

$$A_1 = \begin{vmatrix} A & B \\ 0 & \frac{-1}{\tau_n} \end{vmatrix}$$

$$W_1 = \begin{vmatrix} W & 0 \\ 0 & \frac{V_u}{\tau_n^2} \end{vmatrix} \qquad (1.10)$$

The Kalman filter generates the delayed estimated state $\hat{x}(t-\tau)$ from:

$$\dot{\hat{x}}(t-\tau) = A_1 \hat{x}(t-\tau) + \Sigma_1 C_1^T V_y^{-1} [\, y_p(t) - C_1 \hat{x}(t-\tau) \,] + B_1 u_c(t-\tau) \qquad (1.11)$$

where $C_1 = [C, 0]$, and the error covariance matrix Σ_1 satisfies

$$A_1\Sigma_1 + \Sigma_1 A_1^T + W_1 - \Sigma_1 C_1^T V_y^{-1} C_1 \Sigma_1 = 0 \qquad (1.12)$$

The predictor then generates $\hat{x}(t)$ according to:

$$\hat{x}(t) = \xi(t) + e^{A_1 \tau} [\hat{x}(t-\tau) - \xi(t-\tau)]$$

$$\dot{\xi}(t) = A_1 \xi(t) + B_1 u_c(t) \qquad (1.13)$$

Thus, the human operator model remains linear. Based on man-machine experimental results, each white observation noise v_{y_i} and white motor noise v_u were found to have a covariance proportional to the mean squared values of $E[\, y_i^2 \,]$ and $E[\, u_c^2 \,]$ respectively, i.e.,

$$V_{y_i} = \rho_i \pi \, E[\, y_i^2 \,] \qquad i=1,2,\ldots m$$

$$V_u = \rho_u \pi \, E[\, u_c^2 \,] \qquad (1.14)$$

Therefore, with V_{y_i} is normalized with respect to $E[\, y_i^2 \,]$ with $\rho_i = .01$, it has a positive frequency power density level of -20 db. When V_u is normalized with respect to $E[\, u_c^2 \,]$ with $\rho_u = .003$, it is approximately -25 db. Both of these values have been found to model a variety of simple tracking tasks for a sveral different plants (controlled element dynamics).

2. Past approaches

In the optimal control model of the pilot, therefore, there are some pilot-related model parameters that need to be selected, i.e., weighting of the cost function Q and R, time delay τ , measurement noise v_y and motor noise v_u etc..

There have been some frequency domain methods of experimentally identifying these parameters developed primarily for a compensatory task. In this task only the error signal is displayed to the human controller and therefore only the weighting of error measurement is required. Combined with other model parameters, time delay , measurement noise and motor noise, all have been identified (Ref. 1, 6, 8, 15, 17).

3. Proposed technique

Now we want to identify the optimal control model parameters for pilot performing more complex tasks, and select the weightings of error, error rate, and any other displayed variables appropriate in the task. We may identify the model parameters using both frequency domain and time domain techniques. The former method is a classical approach, and the later is a new one developed by D. K. Schmidt, with emphasis on determining the cost function weightings (Ref. 14). We introduce these two methods as follows.

3.1. Time domain identification

From section 1, we assume

$$\dot{u} = G_x \hat{x} + G_U u - G_U v_U \qquad (3.1)$$

where G_x , G_U are the optimal control gain related to the weighting of cost function J, $\hat{x}$ is the estimate of the state x, and v_U is the motor noise. Let $\epsilon_x = x - \hat{x}$, then

$$\dot{u} = G_x x - G_x \epsilon_x + G_U u - G_U v_U \qquad (3.2)$$

It is assumed that the whole system is stationary and satisfies the ergodic hypothesis. Taking data on u, u, and x from simulation over an appropriate time period, one can obtain

$$\begin{vmatrix} G_x^T \\ G_U^T \end{vmatrix} = [\, M_1 - M_2 \,]^{-1} N_U \qquad (3.3)$$

where

$$M_1 = \begin{vmatrix} E(xx^T) & E(xu^T) \\ E(ux^T) & E(uu^T) \end{vmatrix}$$

$$M_2 = \begin{vmatrix} E(x\epsilon_x^T) & E(xv_u^T) \\ E(u\epsilon_x^T) & E(uv_u^T) \end{vmatrix}$$

$$N_u = \begin{vmatrix} E(xu^T) \\ E(uu^T) \end{vmatrix} \qquad (3.4)$$

Here we note that the estimation error ϵ_x and motor noise v_u are unmeasurable. However we can still proceed with knowledge of the pilot model structure combined with a reasonable assumption on pilot time delay and the covariance of measurement noise and motor noises.

In fact, we can obtain the following relations:

$$E(xv_u) \to 0$$
$$E(u\epsilon_x^T) \approx 0 \qquad (3.5)$$

and approximately we have

$$E(uv_u) \approx \frac{1/2}{\tau_n} V_u = \frac{.005\pi}{\tau_n} E(u_c^2) \qquad (3.6)$$

Here we assume V_u has a normalized value of -20db. $E(x\ \epsilon_x^T)$ can be determined using the properties of the augmented state Kalman filter and a least mean square predictor. That is, since $E(\hat{x}\epsilon_x)=0$,

$$E(x\epsilon_x^T) = E(\epsilon_x\epsilon_x^T) \qquad (3.7)$$

found. We can then find that (Ref. 7), recalling that [ ] = col [x,u]

$$E(\epsilon_\infty \epsilon_\infty^T) = e^{A_1\tau} \Sigma_1 e^{A_1^T\tau} + \int_0^\tau e^{A_1 t} W_1 e^{A_1^T t} dt \qquad (3.8)$$

$$+ \int_0^\infty e^{\bar{A}t} e^{A_1\tau} \Sigma_1 C_1^T V_y^{-1} C_1 \Sigma_1 e^{A_1^T\tau} e^{\bar{A}^T t} dt$$

Here, the A_1, Σ_1, W_1 have been defined in equ. (1.10)-(1.12), and are also functions of $\tau_n (= \frac{-1}{G_U})$, and

$$\bar{A} = \begin{vmatrix} A & B \\ \frac{-L}{\tau_n} & \frac{-1}{\tau_n} \end{vmatrix} \qquad (3.9)$$

We can now use an iterative method in the identification procedure. Try an approximate τ_n to calculate $E(\epsilon_\infty \epsilon_\infty^T)$ used to fit the gain vector $[G_x , G_U]$, then iterate the procedure until the approximated τ_n approaches its fitted value.

The final step is to find the meaningful values of Q and R which corresponds to the experimentally determined optimal gains $[G_x, G_U]$ (see equ. (1.7) and (1.8)). In general the inverse solution is not unique. So in our identification procedure we can arbitrarily choose the weighting on control rate (R) equal to 1, and then use a Quasi-Newton method (see appendix) to identify the other weightings in Q to minimize the modeling error function:

$$J_1 = \sum_{i=1}^{N} \left(\frac{G_{x_i} - \hat{G}_{x_i}}{\sigma_{G_{x_i}}}\right)^2 + \left(\frac{G_U - \hat{G}_U}{\sigma_{G_U}}\right)^2 \qquad (3.10)$$

where G_{x_i} and G_U are estimated mean values, from several of

simulation runs; $\sigma_{G_{x_i}}$, σ_{G_U} are the experimental standard deviations corresponding to each gain; $\hat{G}_{x_i}$,$\hat{G}_U$ are the gains from exercising the model corresponding to some value of Q.

Naturally, this method emphasizes the weightings in the cost function, because we select the time delay,measurement noise, motor noise empirically. We can also select these parameters from the results of the next method, and then compare the results in both approaches.

3.2. Frequency domain identification

First we derive in the frequency domain some characteristic equations from the theoretical pilot optimal control model. From equ. (1.11)-(1.13), we can obtain

$$u_c(s) = L_e\hat{x}(s) = H(s)\ [\ Y(s)+V_y(s)\ ] \qquad (3.11)$$

where

$$L_e = [L,0]$$

$$H(s) = -e^{-s\tau}L_e\ [\ (sI-\hat{A})\int_0^{\tau} e^{(sI-A_1)t}\,dt\ (sI-\bar{A}) + sI-\hat{A}+B_1L_e]^{-1}\ \Sigma_1C_1^TV_y^{-1} \qquad (3.12)$$

with

$$\hat{A} = A_1 - \Sigma_1C_1^TV_y^{-1}C_1 \qquad (3.13)$$

and $\bar{A}$ as in equ. (3.9). Therefore we can consider the pilot model block as Fig. 3-1.

Considering now the pursuit task with single input, in

which the subject observes the input command as well as the system output, (and also their rates implicitly). For example, we take the error e(t), error rate ė(t) , input command i(t) and command rate i̇(t) as our observations (measurements). Then one can consider a closed-loop system , as shown in Fig. 3-2. Referring to the block diagram of Fig. 3-2, we have

$$E(s) = I(s) - M(s)$$

$$M(s) = U(s) \cdot F(s) \qquad (3.14)$$

and

$$U = \frac{1}{\tau_n s+1}[\,(E+N_1)\,H_1 + (sE+N_2)\,H_2 + (I+N_3)\,H_3 + (sI+N_4)\,H_4 + N_u\,] \qquad (3.15)$$

where N_1, N_2, N_3, N_4 and N_u are the measurement noise and motor noises. Here obmiting the symbol (s), we can derive

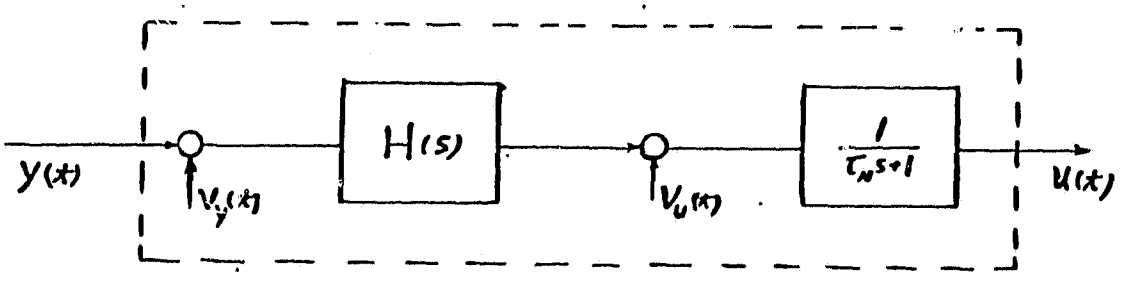

Figure 3-1 Equal pilot OCM model block diagram

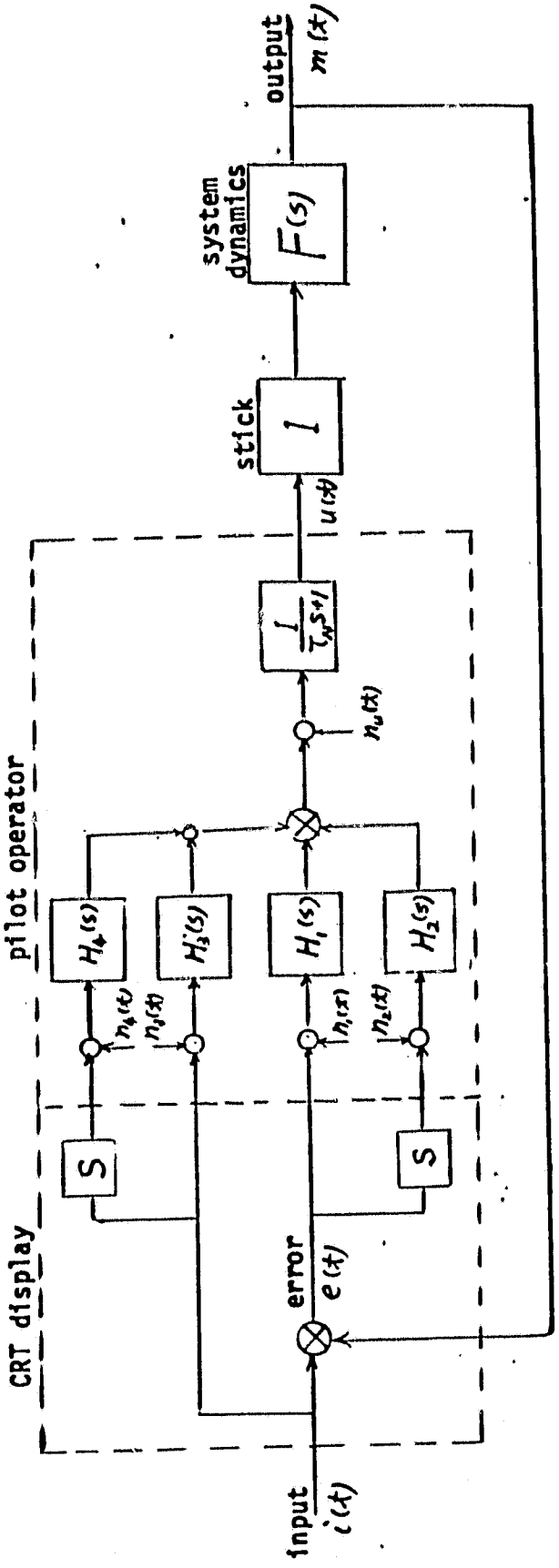

Figure 3-2 Closed-loop system block diagram for pursuit task with single input in OCM model

$$E = \frac{I\left[1. - \frac{F(H_3+sH_4)}{\tau_n s+1}\right] - \frac{F}{\tau_n s+1}\left[H_1N_1+H_2N_2+H_3N_3+H_4N_4+N_U\right]}{1. + \frac{F(H_1+sH_2)}{\tau_n s+1}} \tag{3.16}$$

$$U = \frac{I\left[\frac{H_1+sH_2+H_3+sH_4}{\tau_n s+1}\right] + \frac{1.}{\tau_n s+1}\left[H_1N_1+H_2N_2+H_3N_3+H_4N_4+N_U\right]}{1. + \frac{F(H_1+sH_2)}{\tau_n s+1}} \tag{3.17}$$

Now assume that the system input i(t), measurement noise n_1, n_2, n_3, n_4, and motor noise n_U are uncorrelated with one another. Then we have the following power spectrum relations:

$$\Phi_{iU}(\omega) = \frac{\frac{H_1+sH_2+H_3+sH_4}{\tau_n s+1}}{1 + \frac{F(H_1+sH_2)}{\tau_n s+1}} \Phi_{ii}(\omega) \tag{3.18}$$

$$\Phi_{ie}(\omega) = \frac{1 - \frac{F(H_3+sH_4)}{\tau_n s+1}}{1 + \frac{F(H_1+sH_2)}{\tau_n s+1}} \Phi_{ii}(\omega) \tag{3.19}$$

$$\Phi_{UU}(\omega) = \left|\frac{\frac{H_1+sH_2+H_3+sH_4}{\tau_n s+1}}{1 + \frac{F(H_1+sH_2)}{\tau_n s+1}}\right|^2 \Phi_{ii}(\omega) + \left|\frac{\frac{1.}{\tau_n s+1}}{1 + \frac{F(H_1+sH_2)}{\tau_n s+1}}\right|^2 \left|H_1\right|^2\Phi_{n_1n_1}(\omega) + \left|H_2\right|^2\Phi_{n_2n_2}(\omega) + \left|H_3\right|^2\Phi_{n_3n_3}(\omega) + \left|H_4\right|^2\Phi_{n_4n_4}(\omega) + \Phi_{n_Un_U}(\omega) \tag{3.20}$$

Now we define the equivalent describing function $Y_{P_{eq}}(j\omega)$ as

$$Y_{p_{eq}}(j\omega) = \frac{\Phi_{iu}(\omega)}{\Phi_{ie}(\omega)} \qquad (3.21)$$

Combining equ. (3.18) and (3.19), we have

$$Y_{p_{eq}}(j\omega) = \frac{\Phi_{iu}(\omega)}{\Phi_{ie}(\omega)} = \frac{\dfrac{H_1+sH_2+H_3+sH_4}{\tau_n s+1}}{1-\dfrac{F(H_3+sH_4)}{\tau_n s+1}} \qquad (3.22)$$

which is the same result as Hess' (Ref. 8), with observation of error only in compensatory task (i.e., $H_3=H_4=0$).

We may also define the controller remnant-correlated power spectrum Φ_{uu_r} as the part of the pilot input power spectrum induced by the remnant (measurement noise and motor noise),i.e.,

$$\Phi_{uu_r}(\omega) = \Phi_{uu}(\omega) - \left|\frac{\dfrac{H_1+sH_2+H_3+sH_4}{\tau_n s+1}}{1+\dfrac{F(H_1+sH_2)}{\tau_n s+1}}\right|^2 \Phi_{ii}(\omega)$$

$$= \left|\frac{\dfrac{1}{\tau_n s+1}}{1+\dfrac{F(H_1+sH_2)}{\tau_n s+1}}\right|^2 \Big| |H_1|^2\Phi_{n_1n_1}(\omega)$$

$$+|H_2|^2\Phi_{n_2n_2}(\omega)+|H_3|^2\Phi_{n_3n_3}(\omega)$$

$$+|H_4|^2\Phi_{n_4n_4}(\omega)+\Phi_{n_un_u}(\omega)\Big| \qquad (3.23)$$

Equ. (3.22) and (3.23) are the characteristic equations for a single input pursuit task. Using the same procedure, it can be extended to other complex tasks.

In our certain selection of input command (see section

4), the input power spectrum $\Phi_{ii}(\omega)$ is zero at other than input frequencies. So analyzing the simulation data, we can calculate the equivalent describing function only at the input frequencies, and obtain the controller remnant-correlated power spectrum at other than input frequencies, i.e.,

$$Y_{p_{eq}}(j\omega_k) = \frac{\Phi_{iu}(\omega_k)}{\Phi_{ie}(\omega_k)} \qquad \omega_k = \text{input frequencies}$$

$$\Phi_{uu_r}(\omega_l) = \Phi_{uu}(\omega_l) \qquad \omega_l \neq \text{input frequencies} \qquad (3.24)$$

For computing the power spectrum, we calculate the signals correlation first, and then fast fourier transform it to obtain the power spectrum.

We can identify these model parameters using theoretical modeling to match with the simulation result. For fitting these parameters, we can also include some other important effects which can be obtained during the simulation, such as the variance of pursuit error $E(e^2)$ and the variance of controller $E(u^2)$. Finally we also use Quasi-Newton identification procedure to minimize the modeling error defined below:

$$J_2 = \frac{1}{N_1}\sum_{i=1}^{N_1}\left(\frac{G_i-\hat{G}_i}{\sigma_{G_i}}\right)^2 + \frac{1}{N_2}\sum_{i=1}^{N_2}\left(\frac{P_i-\hat{P}_i}{\sigma_{P_i}}\right)^2 + \frac{1}{N_3}\sum_{i=1}^{N_3}\left(\frac{R_i-\hat{R}_i}{\sigma_{R_i}}\right)^2 + \frac{1}{N_4}\sum_{i=1}^{N_4}\left(\frac{S_i-\hat{S}_i}{\sigma_{S_i}}\right)^2 \qquad (3.25)$$

where

N_i =no. of valid measurement in the i^{th} group
G_i =magnitude of the i^{th} describing function point to be matched, db.
P_i =phase shift of the i^{th} describing function point to be matched, deg.
R_i =controller remnant-correlated power spectrum of the i^{th} frequency point to be matched, db.
S_i = i^{th} variance score to be matched
σ=standard deviation of experimental data
"^": indicates model prediction

4. Simulation with human in the loop

Next we introduce the experimental procedure and the principle of sinusoidal input selection with a simple pursuit task example. During simulation, we generate the data we need for identification. A compensatory task is also done to compare with other results.

4.1. Introduction

The experiment with the pilot in the loop is done in the Flight Simulation Lab., with the use of the minicomputer, CRT, and control stick etc.. In our case, we display the input command i(t) and the system output m(t) on the CRT screen, the human pilot observes the display and determines his command into the control stick, in his attempt to null the error between input command i(t) and system output m(t). Finally the analog signal from the control stick is converted to digital and is input to the dynamic system being simulated numerically by the minicomputer. This closed-loop system with human in the loop is shown in Fig. 4-1, which may be compared to the OCM model already shown in Fig. 3-2. The task to be treated here is the pursuit tracking task with a single input. The CRT and control stick in the lab are shown in Fig. 4-2. Fig. 4-3 shows the CRT display format, in which the distance between line A and line C is the input command i(t), the lines B and C represent system output m(t), and line C is the zero reference line. During our experiment, we simulate two simple systems $\frac{k}{s}$ and $\frac{k}{s^2}$

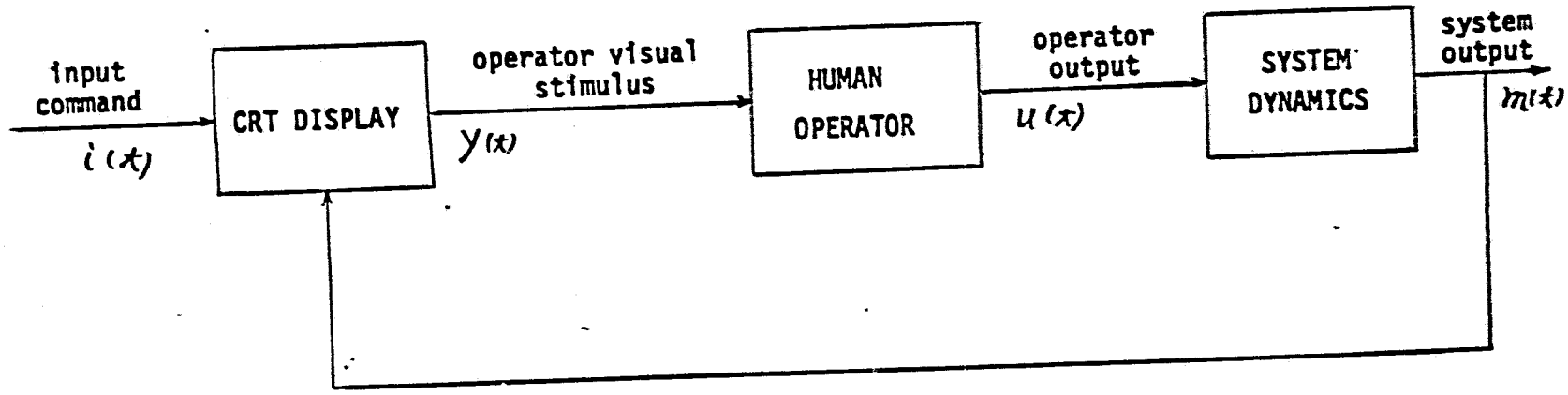

Figure 4-1 Block diagram of closed-loop system with human in the loop

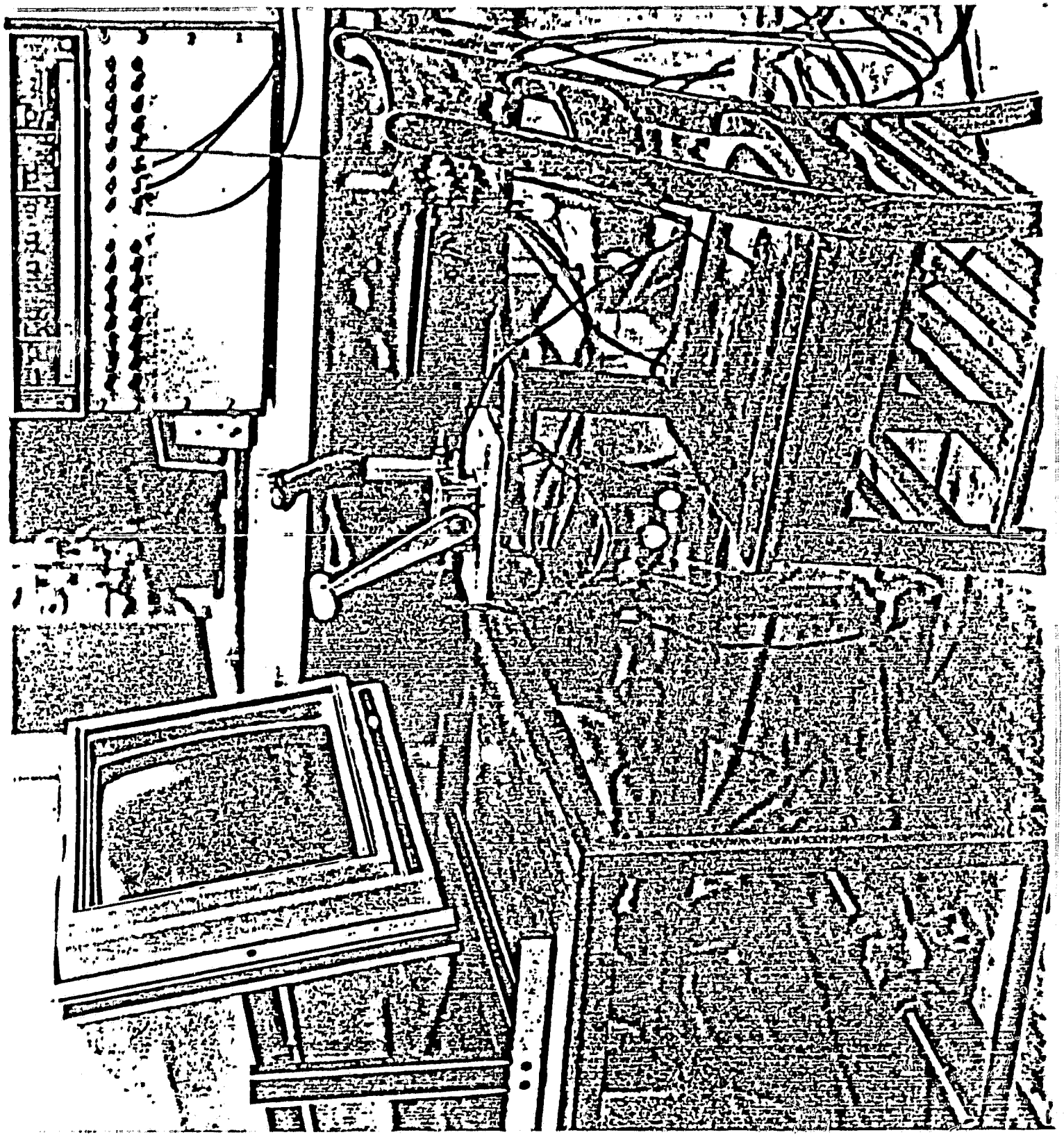

Figure 4-2 Simulation equipment; CRT and control stick

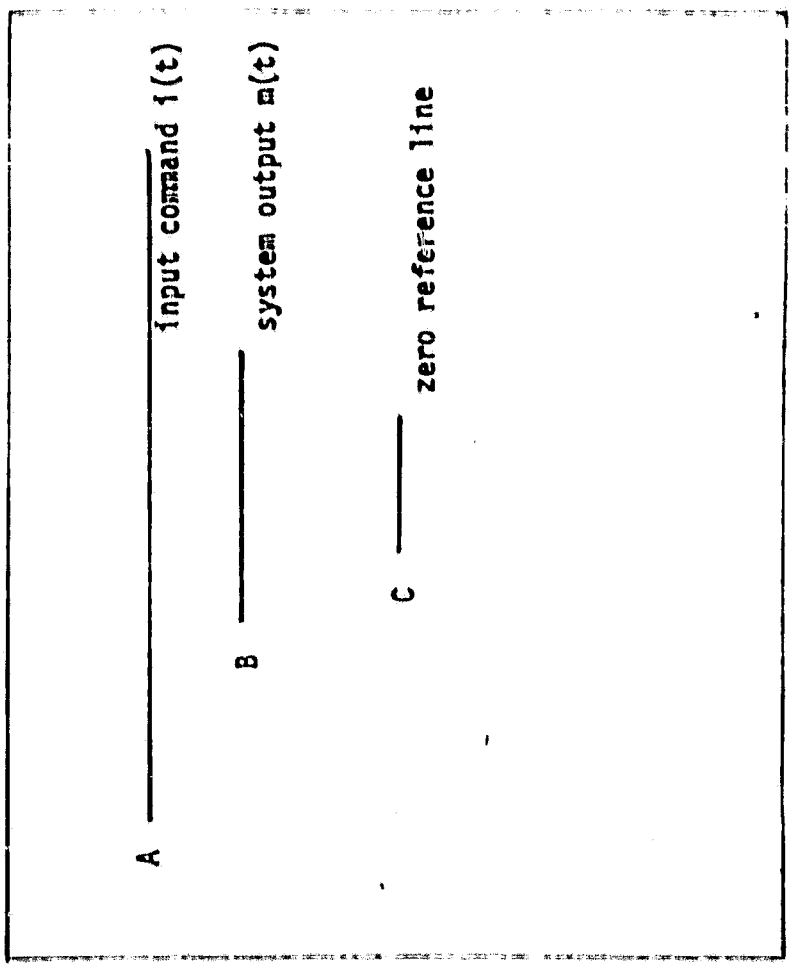

Figure 4-3 CRT display Format

respectively.

4.2. Selection of the sinusoidal input

In the simulation, we use a sinusoidal random-appearing input, mechanized as the sum of sine waves, i.e.,

$$i(t) = \sum_{k=1}^{N} A_k \sin(\omega_k t + \phi_k) \qquad (4.1)$$

Here the ω_k are chosen to be non-commensurable (no frequency is an integral multiple of another), and roughly evenly spaced on a logrithmic scale. In addition the ω_k are selected so that in a finite experimental run length, all the constituent sine waves in i(t) will have completed an integral number of cycles. Finally the ω_k are chosen to lie within the range of interest of human response work, i.e.,

$$0.1 \leq \omega_k \leq 20. \quad \frac{\text{rad}}{\text{sec}} \qquad (4.2)$$

The autocorrelation of the sinusoidal input is

$$\phi_{ii}(\tau) = \sum_{k=1}^{N} \frac{A_k^2}{2} \cos(\omega_k \tau) \qquad (4.3)$$

and its covariance σ_{ii}^2 is

$$\sigma_{ii}^2 = \sum_{k=1}^{N} \frac{A_k^2}{2} \qquad (4.4)$$

So when we use a sinusoidal input as a random-appearing input, we should appropriately select these amplitudes A_k to match the frequency distribution of power in the real random input power spectrum being approximated.

For example, we want to use a sinusoidal input to replace a real random input command θ_c, which satisfies:

$$\begin{vmatrix} \dot{\theta}_c \\ \ddot{\theta}_c \end{vmatrix} = \begin{vmatrix} 0 & 1. \\ -2.25 & -3 \end{vmatrix} \begin{vmatrix} \theta_c \\ \dot{\theta}_c \end{vmatrix} + \begin{vmatrix} 0 \\ 1 \end{vmatrix} w \qquad (4.5)$$

Where w is a white noise ~N(0, 13.5). Taking the Laplace transform:

$$s^2\,\theta_c(s) + 3s\,\theta_c(s) + 2.25\,\theta_c(s) = w(s) \qquad (4.6)$$

or

$$\frac{\theta(s)}{w(s)} = \frac{1.}{(s+1.5)^2} \qquad (4.7)$$

then

$$\Phi_{\theta_c\theta_c}(\omega) = \left|\frac{1.}{(j\omega+1.5)^2}\right|^2 \Phi_{ww}(\omega) = \frac{13.5}{(\omega^2+2.25)^2} \qquad (4.8)$$

To select the sinusoidal input to match the frequency distribution of power with the real random signal, first we define the fraction of power of real random signal $\theta_c(t)$ (Ref. 13) between $0 < \omega$ as

$$F_{\theta_c\theta_c}(\omega) = \frac{\frac{1}{\pi}\int_0^{\omega}\Phi_{\theta_c\theta_c}(\omega)d\omega}{\frac{1}{\pi}\int_0^{\infty}\Phi_{\theta_c\theta_c}(\omega)d\omega} = \frac{\frac{1}{\pi}\int_0^{\omega}\Phi_{\theta_c\theta_c}(\omega)d\omega}{\sigma^2_{\theta_c\theta_c}} \qquad (4.9)$$

And we also define the fraction of power of the sinusoidal input i(t) as

$$F_{ii}(\omega) = \frac{\frac{1}{2}\sum_{k=1}^{n(\omega_n<\omega)} A_k^2}{\frac{1}{2}\sum_{k=1}^{N} A_k^2} = \frac{\frac{1}{2}\sum_{k=1}^{n(\omega_n<\omega)} A_k^2}{\sigma^2_{ii}} \qquad (4.10)$$

Certainly we select $\sigma_{ii}=\sigma_{\theta_c\theta_c}$. Finally, we select the appropriate A_k to match the fraction of power spectrum of sinusoidal input with that of the real random input. It is shown in Fig. 4-4. Table 4-1 shows the parameters selected.

During our system dynamic computation, we choose an integration time interval dt equal to .05 sec and the number of data samples equal to 1024(2^{10}), for the sake of convenience for the fast Fourier transform. The period time T during which data is taken is equal to 51.2 sec, which satisfies the following relation

$$T = N\,\Delta t \qquad (4.11)$$

and define

$$\omega_0 = \frac{2\pi}{T} = .1227185 \quad \frac{\text{rad}}{\text{sec}} \qquad (4.12)$$

We then choose some integers n_k which are non-commensurable to obtain the input frequencies, or

$$\omega_k = n_k\,\omega_0 \qquad (4.13)$$

and ω_k's also are to be equally spaced over the logarithmic scale and satisfies the requirement in equ. (4.2).

4.3. Simulation result

In our experiment, the sinusoidal input shown in Table 4-1 is used to represent a true random input. We simulate two simple plants $\frac{k}{s}$ and $\frac{k}{s^2}$ in both a pursuit and a compensatory task. The results for the pursuit task are shown in Fig. 4-5, 4-6 and Table 4-2 respectively. Fig. 4-7, 4-8 show

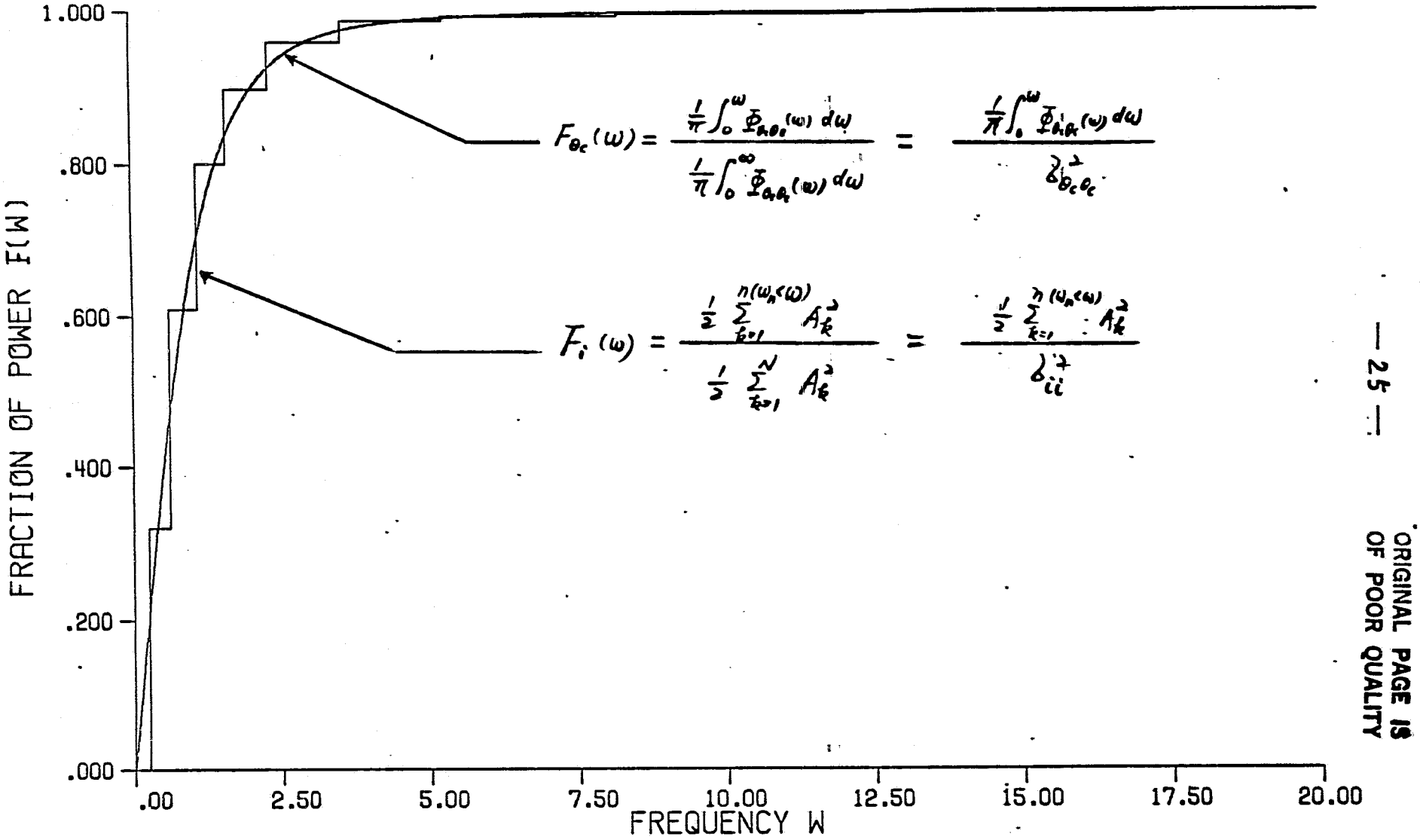

Figure 4-4 Comparison of frequency distribution of power in sum of sine waves with random signal

k	n_k	w_k (rad/sec)	A_k	Φ_k (deg)
1	2	.245437	.80	0.
2	5	.613592	.76	36.
3	9	1.104466	.62	72.
4	13	1.595340	.44	108.
5	19	2.331651	.347	144.
6	29	3.558835	.24	180.
7	43	5.276894	.11	216.
8	67	8.222137	.08	252.
9	101	12.394565	.06	288.
10	-141	17.303303	.06	324.

Table 4-1 Sum of sinusoidal input command

Iterm	k/s dynamics		k/s^2 dynamics	
	mean value	deviation	mean value	deviation
squere of error	.26	.06	.61	.13
square of error rate	4.06	.74	5.08	1.03
square of controller	3.05	.72	26.78	8.65

Table 4-2 Measured human performance

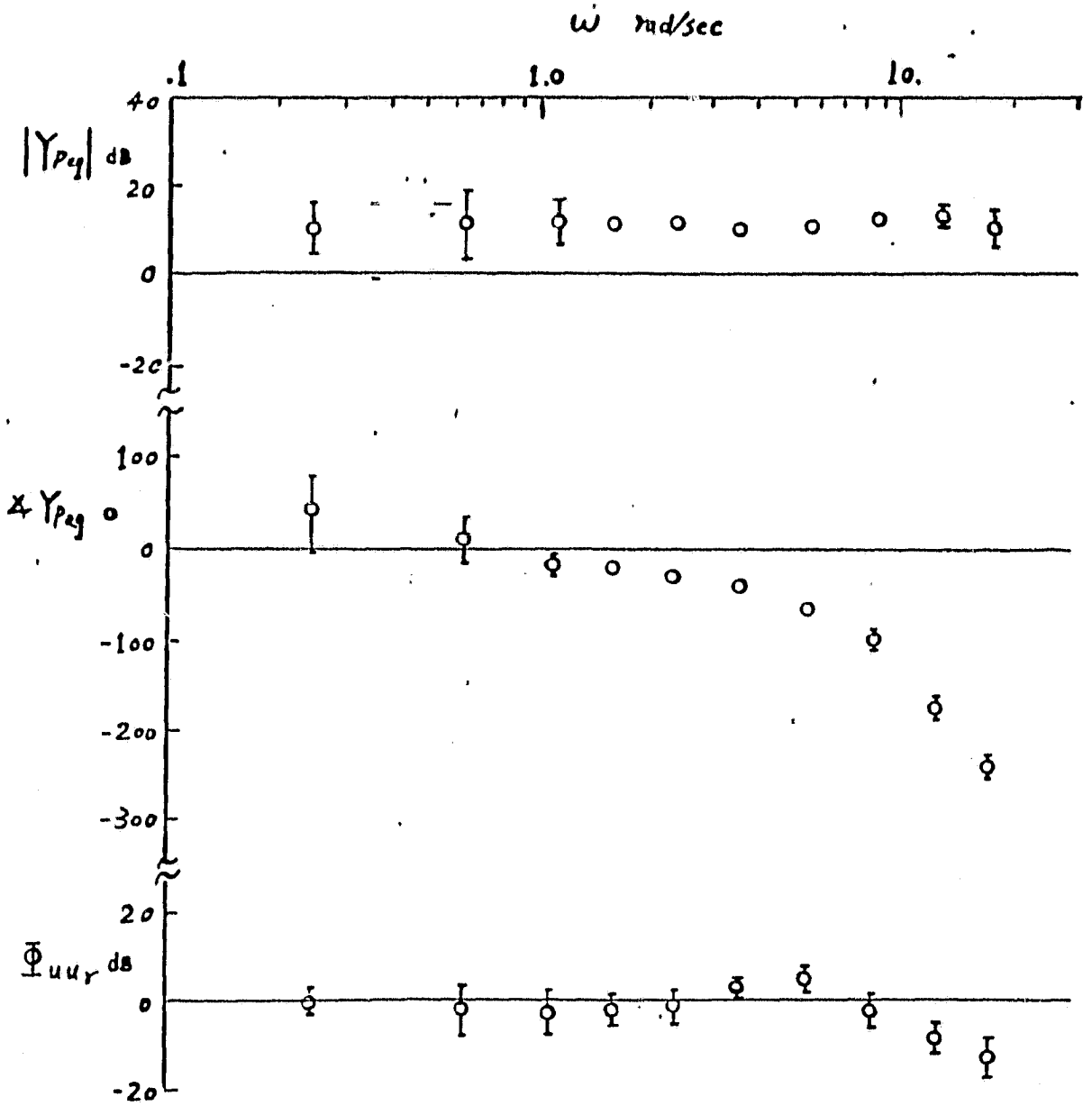

Figure 4-5 Measured human pilot equivalent describing function and controller remnant-correlated power spectrum for k/s dynamics

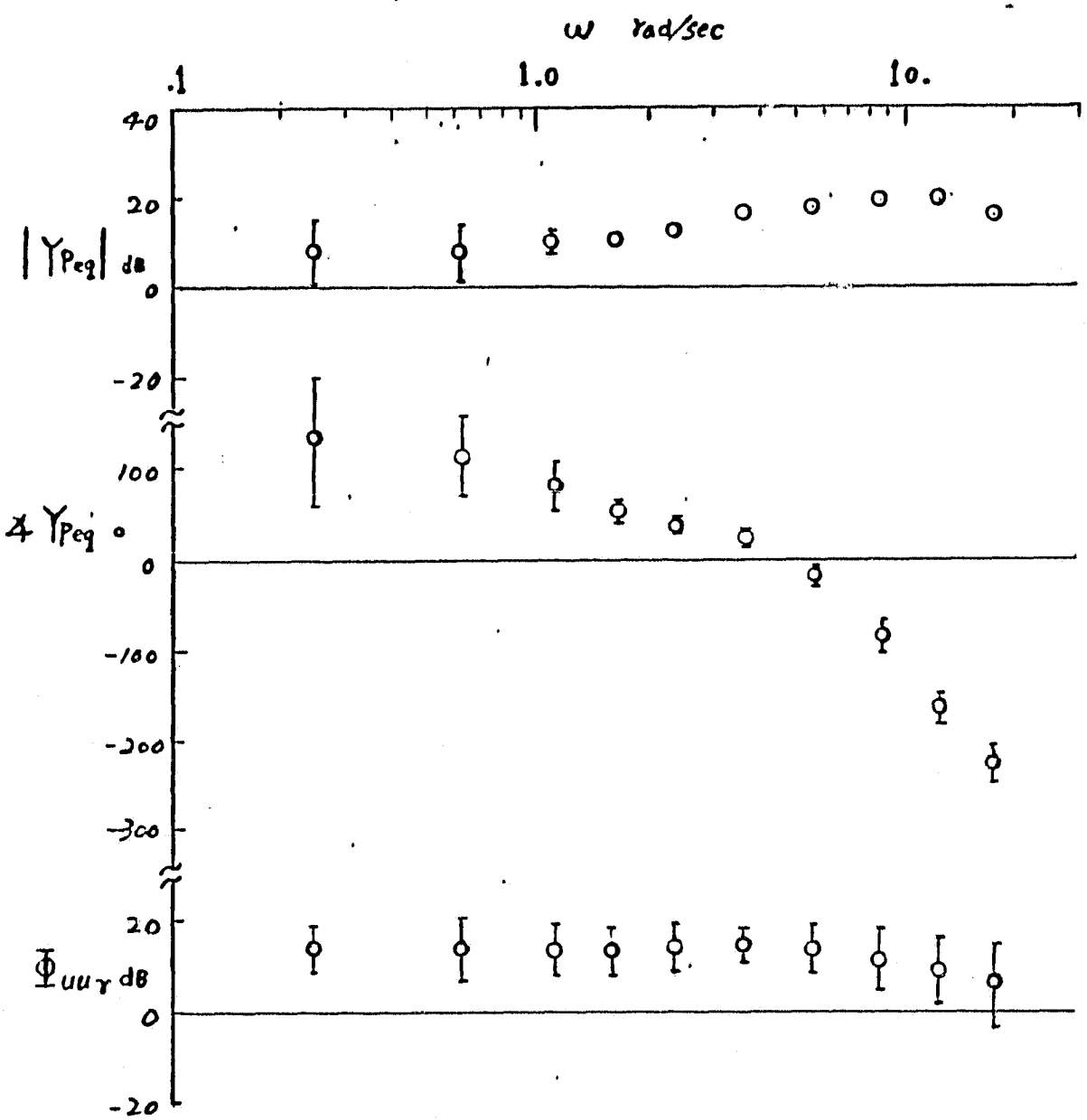

Figure 4-6 Measured human pilot equivalent describing function and controller remnant-correlated power spectrum for k/s^2 dynamics

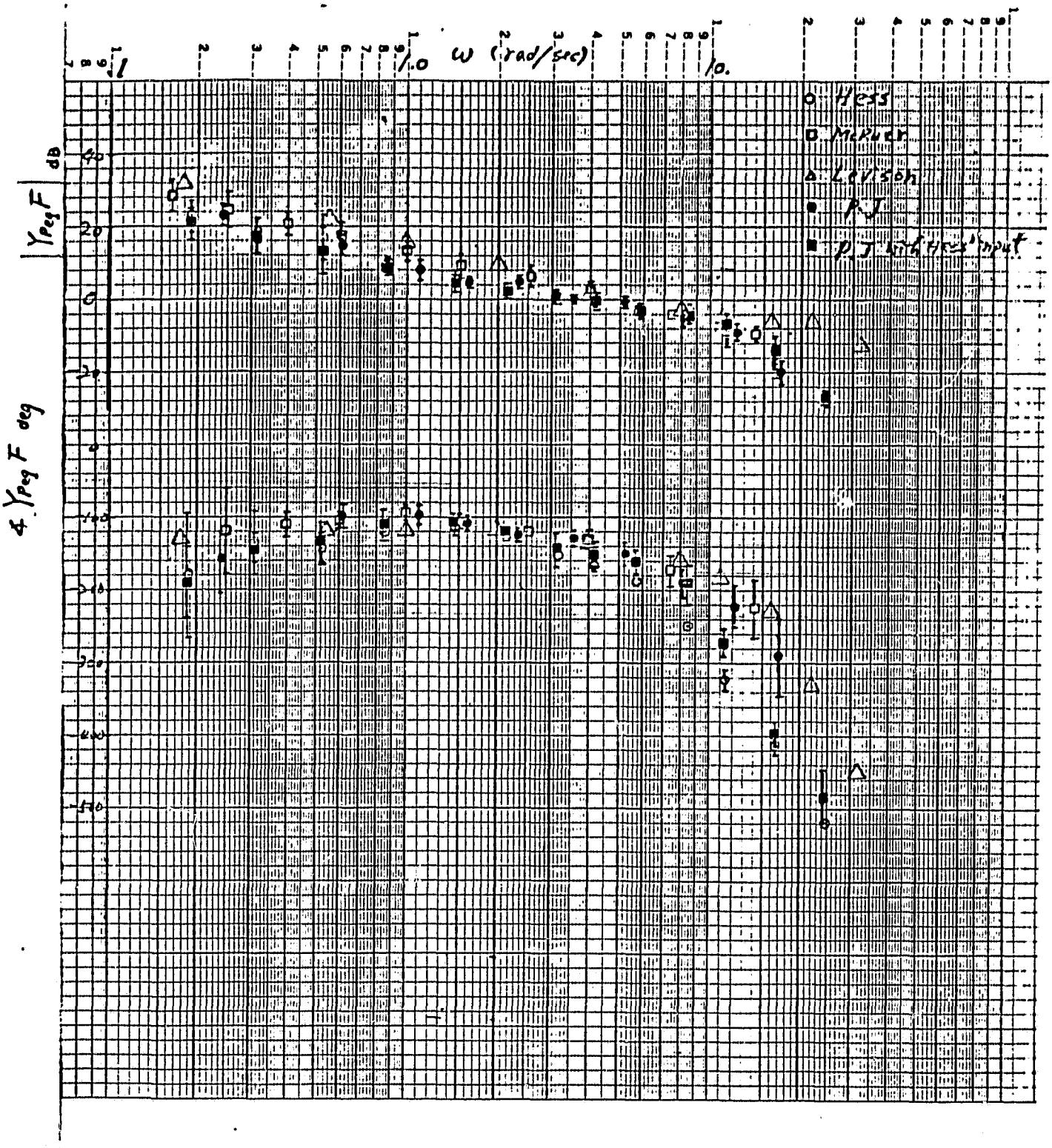

Figure 4-7 Comparison of compensatory task with other results for k/s dynamics

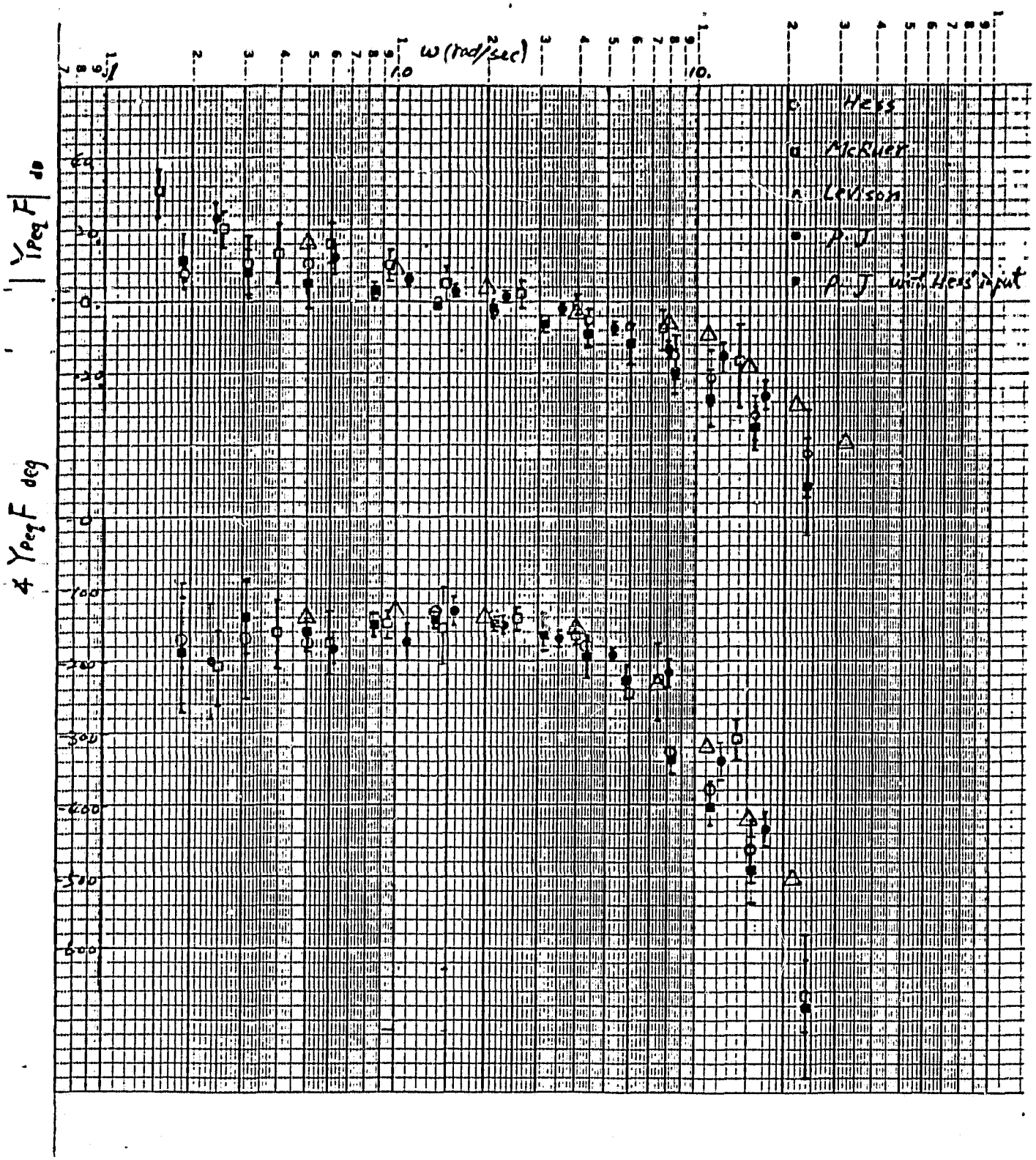

Figure 4-8 Comparison of compensatory task with other results for k/s^2 dynamics

the results for the compensatory task, compared with other results in the literature (Ref. 1,21,22).

From these later results we conclude that our experimental technique and software are correct and that we may proceed to more complex tasks.

4.4. Discussion of Experimental Data

A fixed time interval (.05 sec) and a second order Runge-Kutta integration are used in the real time simulation. The whole discrete closed-loop system is sampled at 20 $\frac{\text{cycle}}{\text{sec}}$ (=125 $\frac{\text{rad}}{\text{sec}}$), which is much larger than our maximum input frequency (=17 $\frac{\text{rad}}{\text{sec}}$). So no aliasing problem is expected for this sampling rate, but at slower rates (say less than 10 $\frac{\text{cycle}}{\text{sec}}$) it must be considered.

Our simulation results shows that there is a little difference between pursuit and compensatory tasks. The magnitude of the pilot describing function is smoother over the whole frequency range in the pursuit task than in the compensatory task. We also have phase lead in the range of low frequencies in the pursuit task, but not in the compensatory task. Also, a lower error variance occurs in the pursuit task, since the subject has more observations, both input and system feedback, and therefore the task is "easier" than the compensatory task.

5. Proposal for further research

We want to identify the pilot dynamics and task objectives (weightings) from simulation data similar to that described, using both time domain and frequency domain methods, and compare the results.

We propose using the Quasi-Newton identification procedure (see appendix) to identify these model parameters, such as weighting of cost function, time delay, measurement noise and motor noise etc..

Our proposed technique can be extended to other more complex tasks, for example, landing approach. During that task, we have more observed variables such as altitude, attitude, angle attack and velocity etc.; and more controllers such as thrust and elevator etc., than those we have in our pursuit task here. Our proposed technique is still available, but more weightibgs of the cost function must be selected, due to the increasing observed variables and controllers.

APPENDIX

A. Quasi-Newton identification procedure (Ref. 15, 16, 17)

A.1 Minimization scheme

The QN scheme is generally implemented to minimize the following scalar modeling error:

$$J = \sum_{i=1}^{N} W_i e_i^2 \qquad (A-1)$$

where e_i is the difference between the i^{th} measured data point and the corresponding model prediction, w_i is a weghting coefficient. Or in matrix form:

$$J = e^T W e \qquad (A-2)$$

with e=col [e_1 e_2 ,...], W=diag [w_i].

For a trial set of model parameters p_1 , we have its corresponding modeling error

$$J_1 = e_1^T W e_1 \qquad (A-3)$$

For a new set of parameters $p_2=p_1+\Delta p$, we obtain a new modeling error

$$\begin{aligned} J_2 &= (e_1+\Delta e)^T W (e_1+\Delta e) \qquad (A-4) \\ &= e_1^T W e_1 + 2 e_1^T W \Delta e + \Delta e^T W \Delta e \end{aligned}$$

Using perturbation theory, we can get approximately linear perturbed equations in the model parameters. Thus

$$\Delta e = Q \, \Delta p \qquad (A-5)$$

where $q(i,j)=\frac{\partial e_i}{\partial p_j}$ can be obtained by the method of perturba-

tion. Now the modeling error can be expressed as

$$J_2 = J_1 + 2e_1^T WQ\Delta p + \Delta p^T Q^T WQ\Delta p \qquad (A-6)$$

Next we want to find the parameter vector change required Δp for minimizing the J_2 . There

$$\frac{\partial J_2}{\partial \Delta p}\Big|_{J_2 \to \text{minimum}} = 0 = 2Q^T We_1 + 2Q^T WQ\Delta p \qquad (A-7)$$

Thus, the following change in the parameter vector yields minimum modeling error, given the initial vector e_1 and the assumption of linearity;

$$\Delta p = - [Q^T WQ]^{-1} Q^T We_1 . \qquad (A-8)$$

A.2 Sensitivity analysis

In addition to obtaining the best match to a given set of data, we may also wish to determine some measure of the reliability of the identified parameter values. A qualitative indication of parameter estimation reliability can often be obtained through sensitivity analysis relating changes in the scalar matching error to perturbations in the model parameters. In general, estimates of parameters that have a high impact on the modeling error can be considered more reliable than estimates of parameters having a smaller impact.

If model predictions are linear in the parameters, as assumed in the foregoing treatment, we may analytically derive the sensitivity of the scalar modeling error to perturbations in model parameters about the optimal (best

matching) set. One may compute the sensitivity to a given parameter with the remaining model parameters held fixed, or with remaining parameters reoptimized. The latter measure provides a more accurate reliability measure because it accounts for the potential tradeoffs that may exist among parameters in terms of matching the data.

Let e_0 be the modeling error when parameter set p is optimized at p_0, then:

$$\Delta p = -[Q^T W Q]^{-1} Q^T W e_0 = 0 \qquad (A-9)$$

Next let us assume that the incremental error arises from a non-optimal choice of one single parameter p_i. With the remaining parameters fixed at their optimal values, the resulting incremental error is

$$\Delta e = q_i \, \Delta p_i \qquad (A-10)$$

where $q_i = i^{th}$ col. of Q. We define the subscript "r" to indicate vectors and matrices that remain when rows and columns corresponding to the i^{th} model parameter are removed. The expressions of re-optimizing the remaining model parameters can be obtained:

$$\Delta p_r = -[Q_r^T W Q_r]^{-1} Q_r^T W q_i \Delta p_i \qquad (A-11)$$

Comparison of the elements of the vector Δp_r with p_i reveals the joint tradeoff between p_i and the remaining model parameters.

To compute the effect on the modeling error J of a change in p_i, with the remaining parameters re-optimized,

we construct a new vector Δp which is the composite of p_i and p_r . This vector is defined as

$$\Delta p = V \Delta p_i \qquad \text{(A-12)}$$

where V is a column vector that has a value of unity for the i^{th} element and values for remaining elements as determined from Δp_r . Then we can obtain the corresponding modeling error for re-optimizing p_r with the change of one single parameter Δp_i

$$\begin{aligned} \Delta J = J - J_o &= 2e_o^T WQV\Delta p_i + V^T Q^T WQV(\Delta p_i)^2 \\ &= V^T Q^T WQV(\Delta p_i)^2 \end{aligned} \qquad \text{(A-13)}$$

The term $2e_o^T WQV\Delta p_i$ is zero, because e_o is corresponding to the optimized modeling error. Therefore the change in modeling error varies as the square of the change in the parameter value. Hence we can obtain the sensitivity for each parameter.

Bibliography

[1] Kleinman, D., Baron, S. and Levison, W. H., "An Optimal Control Model of Human Response parts I and II", Automatica, vol. 6, 1970.

[2] Hess, R. A., "Prediction of pilot opinion ratings using an optimal pilot model", Human factors, vol. 19, 1977.

[3] Schmidt, D. K., "On the use of the OCM's quadratic objective function as a pilot rating metric", presented at 17th Annual Conf. on Manual Control, Los Angles, CA., June 1981.

[4] Schmidt, D. K., "Optimal Flight Control Synthesis Via Pilot Modeling", AIAA J. of Guidance and Control, Vol. 2, No. 4, 1979.

[5] Schmidt, D. K., "Pilot-optimal Augmentation of the Air-to-Air Tracking Task", AIAA J. of Guidance and Control, Vol. 3, No. 5, 1979.

[6] Levison, W. H., Kleinman, D. L. and Baron S., "A model for Human Controller Remnant", IEEE, Trans. Man-Machine System 10, 1969.

[7] Kleinman, D. L., "Optimal linear control for systems with time delay and observation noise", IEEE, Trans. Automatic Control AC-14, 1969.

[8] Hess, R. A., "An introduction to human describing function and remnant measurement in single loop tracking task", AFFDL/FGC-TM-72-9, 1972.

[9] Levison, W. H., Junker, A. M., "Some Empirical Technique for Human Operator Performance Measurement", IEEE, 1980.

[10] Schmidt, D. K., Jones, B. W., "Flight Simulator A+AE Minicomputer System", A+AE Department Document #78-53, school of Aeronautics and Astronautics, Purdue University, 1978.

[11] Bergland, G. D., "A Guided Tour of the Fast Fourier Transform", IEEE Spectrum, July 1969.

[12] Bendat, J. S., Piesol, A. G., "Random data: analysis and measurement procedures", 1971.

[13] Teper, G. L., "An Assessment of the Paper Pilot-an analytical approach to the specification and evaluation of flying qualities", AFFDL-TR-71- 174, June 1972.

[14] Schmidt, D. K., "Time Domain Identification of An Optimal Control Pilot Model with Emphasis on the Objective Function", Presented at the AFFTC/NASA DRYDEN/AIAA Workshop on Flight Test to Identify Pilot Workload and Pilot Dynamics, Edwards AFB, CA., Jan. 1982

[15] Lancraft, R. E. and Kleinman, D. L., "On the Identification of Parameters in the Optimal Control Model", Proceedings of the 15th Annual Conference on Manual Control, Dayton, OH., March 1979.

[16] Levison, W. H., "A Quasi-Newton procedure for Identifying pilot-Related Parameters of the Optimal Control Model", Bolt Beranek and Newman Inc..

[17] Levison, W. H., "Effects of Whole-body Motion Simulation on Flight Skill Development", Report No. 4645, Bolt Beranek and Newman Inc., 1981

[18] Bryson, A. E., Ho, Y. C., "Applied Optimal Control Optimization, Estimation and Control", 1975.

[19] Arthur Gelb, "Applied Optimal Estimation", MIT Press, 1974.

[20] Papoulis, "Probability, Random Variables, and Stochastic Processes", MCGRAW-HILL Series in System Science.

[21] McRuer, D. T., Krendel E. S., "Mathematical Models of Human Pilot Behavior" AGARD-AG-188, Jan. 1974.

[22] Hess, R. A., "The Effects of Time Delays on Systems Subject to Manual Control", NASA 82-1523.